ChemComm

COMMUNICATION

View Article Online
View Journal | View Issue

Cite this: *Chem. Commun.*, 2023, **59**, 4782

Received 27th January 2023,
Accepted 23rd March 2023

DOI: 10.1039/d3cc00382e

rsc.li/chemcomm

Selective photodimerization of acenaphthylene in polymersome nanoreactors†

Sjoerd J. Rijpkema, Sam Vissers and Daniela A. Wilson *

PEG-*b*-PLA polymersomes are used as nanoreactors for the photodimerization of acenaphthylene (ACE), increasing reaction rate significantly. The reaction steered towards almost exclusive formation of *anti* product (94 : 6). This selectivity is remarkable, as other known systems commonly mediate formation of the *syn* product.

A primary goal in the field of artificial nanoreactors is to achieve control over the stereochemistry of a catalytic reaction, a function that natural enzymes exhibit.[1–4] Furthermore, stereochemical photocatalysis in aqueous media is of particular interest due to its sustainable and green impact.[5] However, controlling the stereochemical structure of the product in asymmetric photoreactions is still challenging due to the often highly reactive intermediates[6] which tend to react in any conformation. In recent decades, great effort has been devoted to photocatalytic synthesis.[7,8] However, still few methods are known on controlling stereochemical configuration.

A promising solution to this problem is to template the reactants as a way to force the formation of a single product, similar to enzymes.[9] In the world of supramolecular catalysis many systems have been investigated in the past few decades.[10–12] To this end, scientists have been able to control stereochemistry of photoreactions by creating (supramolecular) reactors,[13] such as organic hosts,[14] metal–organic cages[15–18] and enzyme mimics.[19,20] Intermolecular reactions can be accelerated and controlled due to the immensely increased concentration and the specific orientation of the substrates. Focus on these types of reactors is usually placed on cage-like molecules, while only few examples exist of self-assembled nanoreactors used for photoreactions.[21,22] Our group has developed polymersomes, artificial bilayer vesicles that can be used as nanoreactors, made from biodegradable poly(ethylene glycol)-*b*-poly(D,L-lactide) (PEG-*b*-PLA) block copolymers (Fig. 1A).[23] The block copolymers self-assemble in aqueous solutions into spherical vesicles. Depending

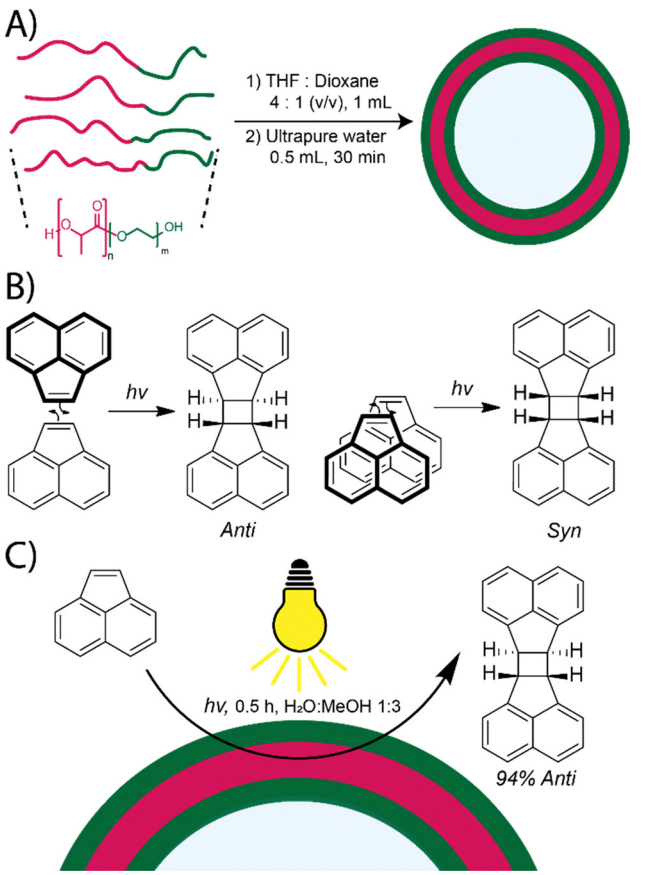

Fig. 1 Schematic of the polymersome nanoreactors. (A) Polymersomes are made *via* self-assembly upon slow addition of water (0.5 mL, 1 mL h^{-1}) to PEG-*b*-PLA in THF/1,4-dioxane (4 : 1 v/v). (B) Photodimerization of acenaphthylene (ACE) can lead to two possible products, *syn* and *anti*. (C) Using UV-light, ACE is selectively converted to the *anti* product *via* insertion into the polymersome membrane.

Department of Systems Chemistry, Institute for Molecules and Materials, Radboud University, Heyendaalseweg 135, 6525 AJ Nijmegen, The Netherlands.
E-mail: d.wilson@science.ru.nl

† Electronic supplementary information (ESI) available. See DOI: https://doi.org/10.1039/d3cc00382e

on the solvent, the membrane of these vesicles can be rigid or flexible.[24,25] By controlling these conditions, the inner membrane of a polymersome can be accessed by substrates.[26] Polymersomes can be applied for the encapsulation of biological compounds,[27,28] mimicking cells,[29] creating artificial organelles,[30] catalysis,[30,31] and for drug delivery.[32–35]

Herein we demonstrate the capabilities of PEG-*b*-PLA polymersomes as a nanoreactor for stereoselective reactions. To investigate the effect of spatial orientation within PEG-*b*-PLA nanostructures on chemical reaction taking place within the membrane, we performed the [2+2] photocycloaddition of acenaphthylene (ACE), a simple and well-known reaction[36] that has been studied in various media yet still desires a high degree of stereo- and regiochemical control.[37] The [2+2] photocycloaddition of olefins is a well-known model photoreaction,[5] but also an important one for natural products synthesis, and drug discovery.[38–40] In this reaction, both the *syn* and *anti* product can be formed based on the orientation of the reactants (Fig. 1B). In our system, we successfully obtained chirality control by the aid of the polymersome membrane without any additional complementary interacting sites or functional groups. Although most nanoreactors in literature facilitate the formation of *syn*, we observed high configurational selectivity for the *anti* form in excellent yield, while the reaction was also accelerated significantly (Fig. 1C).

Three different PEG-*b*-PLA polymers were synthesized using Ring Opening Polymerization (ROP); $mPEG_{22}$-*b*-$PDLLA_{45}$, $mPEG_{22}$-*b*-$PLLA_{45}$ and $mPEG_{22}$-*b*-$PDLA_{45}$. The product compositions were calculated from their respective ^{1}H-NMR and GPC spectra. The polymers were used separately to create two different nanostructures; polymersomes for the atactic and diamond shaped lamellar structures for the isotactic polymers respectively. This was done by dissolving 10 mg of the polymer in organic solvent (THF/1,4-dioxane, 4 : 1 v/v). An equivalent of water was added slowly at 1 mL h^{-1}, inducing self-assembly into spherical polymersomes or lamellar structures as shown by Transmission Electron Microscopy (TEM) (Fig. 2A and B). Shape transformation of polymersomes into somatotypes and rods was also performed in order to apply these morphologies in the dimerization experiments. Shape transformation was performed by dialyzing previously formed polymersomes against a NaCl solution of 10 and 50 mM respectively. The expected morphologies were successfully formed (Fig. 2C and D).

Before performing the photodimerization of ACE in the self-assembled structures, first a suspension of ACE in different solvents was irradiated at 250–385 nm. For quantitative analysis of yield and *syn*/*anti* ratio, quantitative ^{1}H NMR in $CDCl_3$ was applied using 1,3,5-trimethoxy benzene as an internal standard (Fig. S1, ESI†). Results of the control photodimerization reactions are summarized in Table S1 (ESI†). As expected, the reactions proceed poorly. The observed effects of solvent on yield and *syn*/*anti* ratio are in accordance with literature.[41] Long exposure to the light source is required, with little conversion or selectivity.

To perform the reaction with polymersomes present, a suitable solvent is required. This solvent must be able to retain the polymersome structure, as it could redissolve over time if too much organic solvent is used (Fig. S2, ESI†). However, it must also be able to dissolve the ACE. For this reason, a water and methanol mixture was chosen, and the ratio was optimized (Tables S2 and S3, ESI†). The experiments were carried out both with and without polymersomes present, and were irradiated for 15 minutes. Water has a smaller effect on the glass transition temperature (T_g) of PEG-*b*-PLA compared to organic solvents, thus making the membrane less permeable.[42] It is also not a good solvent for ACE, driving it into the membrane. Methanol can still keep the polymersome structure stable, but lowers the T_g significantly to around 5 °C (Fig. S3, ESI†), making the membrane more flexible at room temperature so ACE can enter it (Fig. S4, ESI†). It is however also a good solvent for ACE, which could keep the substrate in solution instead of in the membrane. As expected, we found almost no yield in pure water and methanol. This can be explained as only water does not solubilise ACE, making it unable to undergo the reaction. Our PEG-*b*-PLA is also known to have a T_g slightly above room temperature in water, explaining why the substrate cannot enter the membrane.[43] In pure methanol, ACE stays dissolved instead of entering the membrane, thus similar results are found compared to the absence of polymersomes. We found that for a methanol content between 25–75% in water, the yield is increased significantly when polymersomes were present. Without polymersomes, only a small increase in yield was observed together with a preference towards the *syn* product.

To prove that ACE can enter the PLA membrane of the polymersomes when methanol is present, ^{1}H NMR kinetics experiments were conducted. If exchange of ACE between the solution and polymersomes would occur, the T_1 relaxation should decrease when polymersomes are added, as the membrane disturbs the

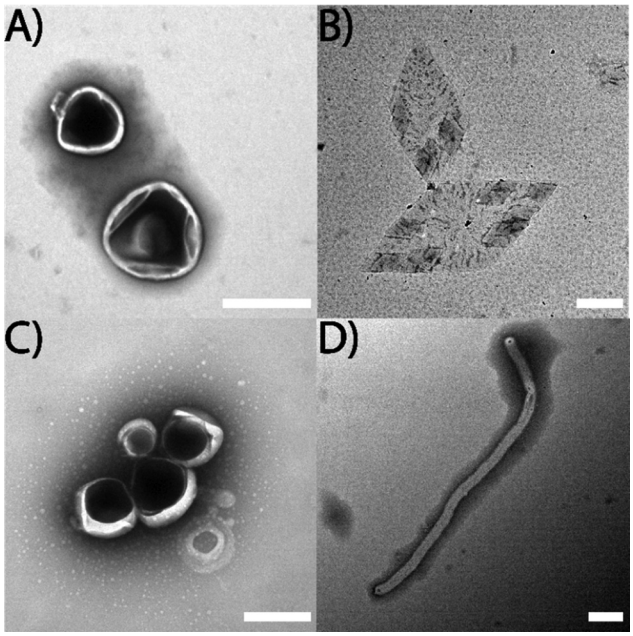

Fig. 2 TEM images $mPEG_{22}$-*b*-$PDLLA_{45}$ (A) polymersomes and $mPEG_{22}$-*b*-$PLLA_{45}$ (B) lamellar structures. Shape transformation of the polymersomes yielded (C) stomatocytes and (D) rods. Staining was used to make the structures more visible on TEM (A, C and D). Scale bar: 500 nm.

magnetization of ACE during exchange.[44] T_1 was measured for ACE with and without a 5 mg mL^{-1} polymersome solution in $CD_3OD:D_2O$ 3 : 1 at 40 °C. It was found that the T_1 relaxation of ACE in solution was 9.0 s, while with polymersomes present this number decreased to 1.4 s, indicating a rapid exchange with the polymersome membrane (Fig. S5, ESI†). Additionally, we followed the conversion of ACE over time with PEG-*b*-PLA polymersomes present (Fig. S6, ESI†). When PEG-*b*-PS polymersomes were added instead, which do not allow the substrate to enter the membrane, no conversion was observed (Fig. S7, ESI†).

When a water/methanol ratio of 25/75 is used as solvent with polymersomes present, we found that the reaction was driven towards almost exclusive formation of *anti* product. *anti* formation typically occurs when heavy atom solvents are added, due to an increased population of triplet states.[37,40,41] Comparing the samples with and without polymersomes present, it is clear that the polymersome drives the reaction towards the *anti* product. The reaction in 25/75 H_2O/MeOH was then tracked over time to investigate the speed of the formation of ACE dimer over time. The result is displayed in Table S4 (ESI†). Conversion plateaued after 30 minutes of irradiation, which is significantly faster than the reaction in solvent, and even compared to other nanocages.[21,45–49]

Finally, we used a variety of morphologies to investigate what influence they held over the reaction, as seen in Table S5 (ESI†). It can be concluded that the morphology has no influence on the photodimerization reaction in the presence of mPEG-*b*-PLA nanostructures. It was found that the different morphologies of $mPEG_{22}$-*b*-$PDLLA_{45}$; polymersomes, stomatocytes and rods, all gave similar outcomes. Also by using a more tactic polymer, similar conversion was obtained. However, if PEG-*b*-PS polymersomes are applied, the high conversion and *anti* selectivity is not observed anymore. The T_g of PS is significantly higher than that of PLA, making it harder for substrate to enter the membrane, showing the necessity of PLA in this reaction.[24] The reaction appears to proceed mostly in solution in this system, resulting in comparable observations to that of the reaction in solvent. An overview of the reactions is given in Table 1.

Table 1 Summary of photodimerization results for different systems, irradiated for 30 minutes

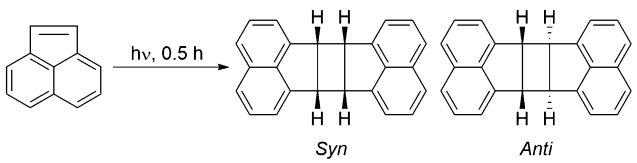

Medium	Conversion%	*anti*%	*syn*%
H_2O	0	—	—
MeOH	15.5	24.0	76.0
25 : 75 H_2O : MeOH	30.8	26.9	73.1
$mPEG_{22}$-*b*-$PDLLA_{45}$ polymersomes 25 : 75 H_2O : MeOH	82.2	94.1	5.9
$mPEG_{44}$-*b*-PS_{176} polymersomes 25 : 75 H_2O : MeOH	31.2	20.6	79.4

The product formed during the photodimerization is highly dependent on a number of factors. Increased local concentration greatly enhances yield, and the excited singlet state yields the *syn* dimer while the triplet state yields both *syn* and *anti* dimers, with the latter as the major product.[41,50] It is well known that in organic solvents the ratio of *syn* to *anti* dimers, apart from the concentration of acenaphthylene, depends on the formation of singlet or triplet excited states. Since we perform this reaction under an argon atmosphere, no oxygen is present to quench the triplet state. Depending on the solvent polarity, the acenaphthylene triplet can give both *syn* and *anti* dimers. A high polarity results in increased stabilization of the transition state leading to the *syn* dimer, while lower polarity leads to the *anti* dimer.[41] The inner membrane of the polymersome is hydrophobic, and we believe this can provide an environment in which dimerization is driven towards *anti* product formation. This is contrary to other nanoreactors used throughout literature to optimize this reaction, which mainly result in *syn* formation.[21,47–49] For instance nano-cages[51] and sodium dodecyl sulfate micelles[52] can also provide a fast conversion, but with high selectivity only for the *syn* product. In dendrimeric systems[53] and nanocapsules,[54] this conversion can take up to 12 hours. In some systems, space constraints are used to align ACE in a favorable position to for the *syn* or *anti* variant. For example, in γ-cyclodextrin thioethers the cavity hosts two ACE molecules which can only react to exclusively form the *anti* product.[54,55] Though effective, these reactions take many hours and only get a very low conversion (<29%). Comparatively, our polymersome nanoreactor can form the *anti* product near selectively in 30 minutes.

In conclusion, we have shown PEG-*b*-PLA self-assembled nanostructures can be used as reactors to promote intermolecular [2+2] photodimerization of acenaphthylene. By varying the solvent, reaction time and nanostructure we have been able to optimize the selectivity of the reaction. By performing the reaction in 3 : 1 MeOH : H_2O, the reaction rate is increased significantly as membrane of the mPEG-*b*-PLA nanostructures become accessible to the substrate. Specifically, the reaction is steered towards almost exclusive formation of *anti* product with a 94% *anti* formation over *syn* and a total yield of 82%, not yet seen before in literature. We believe selectivity and enhanced reactivity during direct excitation can be attributed to the hydrophobic membrane of the nanoreactor, which localizes the substrate and enhances *anti* formation. This selectivity is remarkable compared to other systems used in the photocatalysis of ACE, which commonly mediate the formation of *syn* product.

Conflicts of interest

There are no conflicts to declare.

Notes and references

1 C. J. Brown, F. D. Toste, R. G. Bergman and K. N. Raymond, *Chem. Rev.*, 2015, **115**(9), 3012–3035.
2 M. Raynal, P. Ballester, A. Vidal-Ferran and P. W. N. M. van Leeuwen, *Chem. Soc. Rev.*, 2014, **43**(5), 1734–1787.

3 S. H. A. M. Leenders, R. Gramage-Doria, B. de Bruin and J. N. H. Reek, *Chem. Soc. Rev.*, 2015, **44**(2), 433–448.
4 M. Otte, *ACS Catal.*, 2016, **6**(10), 6491–6510.
5 V. Ramamurthy and J. Sivaguru, *Chem. Rev.*, 2016, **116**(17), 9914–9993.
6 C. Yang, *Chin. Chem. Lett.*, 2013, **24**(6), 437–441.
7 Y. Xu, M. L. Conner and M. K. Brown, *Angew. Chem., Int. Ed.*, 2015, **54**(41), 11918–11928.
8 S. Poplata, A. Tröster, Y.-Q. Zou and T. Bach, *Chem. Rev.*, 2016, **116**(17), 9748–9815.
9 N. Vallavoju and J. Sivaguru, *Chem. Soc. Rev.*, 2014, **43**(12), 4084–4101.
10 M. Morimoto, S. M. Bierschenk, K. T. Xia, R. G. Bergman, K. N. Raymond and F. D. Toste, *Nat. Catal.*, 2020, **3**(12), 969–984.
11 Z. Wang, M. C. M. van Oers, F. P. J. T. Rutjes and J. C. M. van Hest, *Angew. Chem., Int. Ed.*, 2012, **51**(43), 10746–10750.
12 F. P. Ballistreri, R. M. Toscano, M. E. Amato, A. Pappalardo, C. M. A. Gangemi, S. Spidalieri, R. Puglisi and G. Trusso Sfrazzetto, *Catalysts*, 2018, **8**(4), 129.
13 T. S. Koblenz, J. Wassenaar and J. N. H. Reek, *Chem. Soc. Rev.*, 2008, **37**(2), 247–262.
14 C. Yang and Y. Inoue, *Chem. Soc. Rev.*, 2014, **43**(12), 4123–4143.
15 D. Preston, J. J. Sutton, K. C. Gordon and J. D. Crowley, *Angew. Chem., Int. Ed.*, 2018, **57**(28), 8659–8663.
16 W. Cullen, H. Takezawa and M. Fujita, *Angew. Chem., Int. Ed.*, 2019, **58**(27), 9171–9173.
17 I. Sinha and P. S. Mukherjee, *Inorg. Chem.*, 2018, **57**(8), 4205–4221.
18 Y. Nishioka, T. Yamaguchi, M. Kawano and M. Fujita, *J. Am. Chem. Soc.*, 2008, **130**(26), 8160–8161.
19 D. B. Singh, *Chem. Sci. J.*, 2018, **9**(3), 1000192.
20 M. J. Wiester, P. A. Ulmann and C. A. Mirkin, *Angew. Chem., Int. Ed.*, 2011, **50**(1), 114–137.
21 S. Dawn, S. R. Salpage, B. A. Koscher, A. Bick, A. C. Wibowo, P. J. Pellechia and L. S. Shimizu, *J. Org. Chem.*, 2014, **118**(45), 10563–10574.
22 D. G. Shchukin and D. V. Sviridov, *J. Photochem. Photobiol., C*, 2006, **7**(1), 23–39.
23 B. J. Toebes, L. K. E. A. Abdelmohsen and D. A. Wilson, *Polym. Chem.*, 2018, **9**(23), 3190–3194.
24 S. J. Rijpkema, B. J. Toebes, M. N. Maas, N. R. M. de Kler and D. A. Wilson, *Isr. J. Chem.*, 2019, **59**(10), 928–944.
25 Y. Men, W. Li, C. Lebleu, J. Sun and D. A. Wilson, *Biomacromolecules*, 2020, **21**(1), 89–94.
26 M. C. M. van Oers, L. K. E. A. Abdelmohsen, F. P. J. T. Rutjes and J. C. M. van Hest, *Chem. Commun.*, 2014, **50**(31), 4040–4043.
27 M. Nijemeisland, L. K. E. A. Abdelmohsen, W. T. S. Huck, D. A. Wilson and J. C. M. van Hest, *ACS Cent. Sci.*, 2016, **2**(11), 843–849.
28 F. Du, S. Bobbala, S. Yi and E. A. Scott, *J. Controlled Release*, 2018, **282**, 90–100.
29 E. Rideau, R. Dimova, P. Schwille, F. R. Wurm and K. Landfester, *Chem. Soc. Rev.*, 2018, **47**(23), 8572–8610.
30 H. Che and J. C. M. van Hest, *ChemNanoMat*, 2019, **5**(9), 1092–1109.
31 K. Renggli, P. Baumann, K. Langowska, O. Onaca, N. Bruns and W. Meier, *Adv. Funct. Mater.*, 2011, **21**(7), 1241–1259.
32 S. Jo, F. R. Wurm and K. Landfester, *Nano Lett.*, 2020, **20**(1), 526–533.
33 J. Li, Y. Li, Y. Wang, W. Ke, W. Chen, W. Wang and Z. Ge, *Nano Lett.*, 2017, **17**(11), 6983–6990.
34 T. Nishimura, Y. Sasaki and A. Akiyoshi, *Adv. Mater.*, 2017, **29**, 1702406.
35 J. Li, Y. Anraku and K. Kataoka, *Angew. Chem., Int. Ed.*, 2020, **59**, 13526.
36 E. J. Bowen and J. D. F. Marsh, *J. Chem. Soc.*, 1947, 109–110.
37 N. Haga, H. Takayanagi and K. Tokumaru, *J. Org. Chem.*, 1997, **62**(11), 3734–3743.
38 X. Huang, T. R. Quinn, K. Harms, R. D. Webster, L. Zhang, O. Wiest and E. Meggers, *J. Am. Chem. Soc.*, 2017, **139**(27), 9120–9123.
39 R. Brimioulle and T. Bach, *Science*, 2013, **342**(6160), 840–843.
40 N. Vallavoju, S. Selvakumar, S. Jockusch, M. P. Sibi and J. Sivaguru, *Angew. Chem., Int. Ed.*, 2014, **53**(22), 5604–5608.
41 D. O. Cowan and R. L. E. Drisko, *J. Am. Chem. Soc.*, 1970, **92**(21), 6286–6291.
42 S. A. Meeuwissen, K. T. Kim, Y. Chen, D. J. Pochan and J. C. M. van Hest, *Angew. Chem., Int. Ed.*, 2011, **50**(31), 7070–7073.
43 A. C. Apolináro, M. S. Magoń, A. Pessoa Jr. and C. D. O. Rangel-Yagui, *Nanomaterials*, 2018, **8**, 373.
44 S. Forsén and R. A. Hoffman, *J. Chem. Phys.*, 1963, **39**(11), 2892–2901.
45 D. O. Cowan and J. C. Koziar, *J. Am. Chem. Soc.*, 1974, **96**(4), 1229–1230.
46 D. O. Cowan and R. L. E. Drisko, *J. Am. Chem. Soc.*, 1970, **92**(21), 6281–6285.
47 J. Guo, Y.-Z. Fan, Y.-L. Lu, S.-P. Zheng and C.-Y. Su, *Angew. Chem., Int. Ed.*, 2020, **59**(22), 8661–8669.
48 V. Ramamurthy, D. R. Corbin, C. V. Kumar and N. J. Turro, *Tetrahedron Lett.*, 1990, **31**(1), 47–50.
49 E. E. Karslyan, A. I. Konovalov, A. O. Borissova, P. V. Petrovskii and A. R. Kudinov, *Mendeleev Commun.*, 2012, **22**(4), 189–191.
50 R. Livingston and K. S. Wei, *J. Phys. Chem.*, 1967, **71**(3), 541–547.
51 M. Yoshizawa, Y. Takeyama, T. Kusukawa and M. Fujita, *Angew. Chem., Int. Ed.*, 2002, **41**(8), 1347–1349.
52 H. Mayer and J. Sauer, *Tetrahedron Lett.*, 1983, **24**(38), 4091–4094.
53 L. S. Kaanumalle, R. Ramesh, V. S. N. Murthy Maddipatla, J. Nithyanandhan, N. Jayaraman and V. Ramamurthy, *J. Org. Chem.*, 2005, **70**(13), 5062–5069.
54 L. S. Kaanumalle and V. Ramamurthy, *Chem. Commun.*, 2007, 1062–1064.
55 H. M. Wang and G. Wenz, *Beilstein J. Org. Chem.*, 2013, **9**, 1858–1866.